Eugeniusz KURGAN
AGH University of Science and Technology

Numerical computation of mutual force acting between two particles in DC dielectrophoresis

***Abstract**: Dielectrophoresis, arising from spatially nonuniform electric fields, has become one of the more promising tools for particle manipulation in microfluidics and nanofluidics. Dielectrophoresis is the translational motion of neutral matter caused by polarization effects in a non-uniform electric field. It is considered force acting on two particles placed close each other an influence of mutual distance between them on this force has been discussed. Nonuniform field with high gradient has been obtained by two electrodes polarised by DC potential. Laplace's partial differential equation was solved by finite element method. Surface stress densities was calculated by Maxwell stress method on both sides of the particle surface and next integrate on this surface giving total force acting on particle.*

***Streszczenie.** Ponieważ środowisko obliczeniowe jest liniowe, niejednorodne i izotropowe, to do obliczenia rozkładu potencjału zostanie użyte również i w tym przypadku równanie Laplace'a i rozwiązane ono zostanie metodą elementów skończonych trójkątnych z sześcienną aproksymacją niewidomej w każdym elemencie. Naprężania powierzchniowe po obu stronach powierzchni cząsteczki liczone jest metodą naprężeń Maxwella, a następnie całkowane po całej powierzchni cząsteczki, po to aby otrzymać całkowitą siłę działającą na cząsteczkę. (**Obliczenia numeryczne siły wzajemnej między dwoma cząstkami w dielektroforezie DC**)*

Keywords: dielectrophoresis, dipole force calculations, Maxwell stress method
Słowa kluczowe: dielektroforeza, siły działających na dipol, metoda naprężeń Maxwella.

Introduction

It is well-known that an electrically neutral but polarizable particle, suspended in a dielectric or conducting fluid, under the influence of a non-uniform electric field tends to move towards the region of highest electric field intensity. This migration caused by dielectric polarization forces is discovered by [2] and named as dielectrophoresis. During the past years dielectrophoresis has proved to be of very important in many applications such as, for example, industrial filtration of liquids, dielectric solid - solid separations and biological analyses.

In comparison to electrophoresis, by which we understand particle motion due to the force resulting from coupling between an applied external electric field and a charge particle, dielectrophoresis has the disadvantage that the polarization forces acting on polarized particle are quite weak. In general, efficient particle manipulation in microelectrode arrangement requires taken into account other factors, such as viscous, buoyancy, and electrohydrodynamic forces.

There are many reasons for studying a behavior of particles and fluid globules immersed fluid suspension and placed in electric fields. Among different the chemical engineering applications [3] are the determination of forces acting on droplets exiting electrospray nozzles, the enhancement of heat and mass transfer in emulsions by the imposition of electric fields [3], electrically driven separation of particles techniques, dielectrophoretic and electrorotational manipulation of living and death cells, and the control of electrorheological fluids.

The calculation of DEP force acting on particle has been reported as a difficult task unless in many cases simplifying assumptions and very simple geometries are considered and is usually based on the dipole approximation first introduced by Pohl [1]. Pohl derived an expression for the dielectrophoretic force acting on cells by modeling the cell as a solid spherical dielectric particle placed in a fluid medium. A more realistic geometries for biological particles has been used by a number of scientists, which includes a spherical dielectric shell employed usually for the dielectric properties of the plasma-membrane.

Dielectrophoretic (DEP) traps use the force acting on an induced multipole with a nonuniform steady or alternating electric field to create electric forces that will change position of particles. DEP forces can trap different kind of particles on or between special electrodes – among others including micron and submicron polymer beads, cells, viruses, and bacteria. With the appropriate electrode geometry design and careful control of the potentials conditions, single particle trapping can be attained [4].

The Finite Element Method (FEM) is useful method for analysing electromagnetic fields in devices, because these can model complicated geometries and non-linear electric properties with relatively short computing time. In spite of these advantages, in many papers have been proved that obtaining an accurate force or torque from FEM computation can be inaccurate, particularly when geometry is enough complex, such as in the case of dielectrophoretic traps with multiple particles [5]. Unfortunately, force and torque calculations are influenced by the approximate nature of the discretisation used in FEM meshes.

In this paper it is considered force acting on two particles placed close each other an influence of mutual distance between them on this force has been discussed. Nonuniform field with high gradient has been obtained by two electrodes polarised by DC potential. Laplace's partial differential equation was solved by finite element method. Surface stress densities was calculated by Maxwell stress method on both sides of the particle surface and next integrate on this surface giving total force acting on particle.

Equations describing the electromagnetic field

In practical applications of dielectrophoresis, inhomogeneous electric filed with sufficient gradient is obtained throughout adequate configuration of electrode geometry of the channel, where particles in dielectric fluid are moving and by properly little electrode dimensions. Important role plays here sharp edges of electrodes, where in vicinity of them, as it is commonly known, electric field attains high values and with high gradients. In order to orientate about size of errors, which introduce equivalent dipole method and numerical method used to solve adequate Laplace's equation on size of occurring here errors, it is necessary to know exact solution of the electromagnetic field and its gradients in computational domain [6]. When geometrical shapes of electrodes and fluid flow channel have complicated shapes, it is very difficult to solve analytically Laplace's equation together with, frequently, complicated boundary conditions [7]. Inhomogeneous field with arbitrary shape, can be relatively easy obtained in inhomogeneous medium, with very simple geometrical shape of computational domain.

Let us assume that geometrical form of channel has a cuboid shape with following dimensions: L in direction of x-axis, h in direction in y-axes and $L_p = 1\mathrm{m}$ in z-axis. Two dimensional cross section of the channel with dielectric fluid, but without a particle, is presented in Fig. 1. On this figure we have the two particle of the same radius and dielectric permitivity.

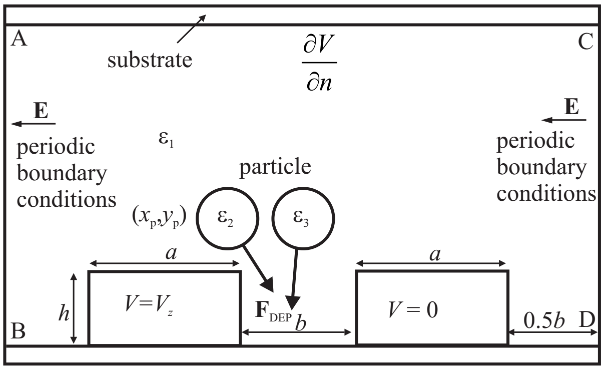

Fig.1. Inhomogeneous medium without a particle.

Now we assume following computational data: segment $AB = CD = h = 40\mu\mathrm{m}$, $BD = AC = L = 100\mu\mathrm{m}$, the left particle radius $r_0 = 3\mu\mathrm{m}$ and it is placed at point $x_p = 40\mu\mathrm{m}$ and $y_p = 10\mu\mathrm{m}$ and right particle radius $r_0 = 3\mu\mathrm{m}$ and it is placed at point $x_p = 46.5\mu\mathrm{m}$ and $y_p = 10\mu\mathrm{m}$. On side AB there are zero boundary conditions and on side CD potential is constant and is equal $V_z = 10\mathrm{V}$. On segments BD and AC normal derivative of the potential V perpendicular to boundary amounts zero. It was assumed that relative permittivity of the fluid $\varepsilon_1 = 5$, and both particles $\varepsilon_2 = \varepsilon_3 = 50$. On the Fig.1 two segments KL and MN are distinguished along which we shell observe analyzed values.

Polarizations on surfaces of both particles are given by

(1) $$\mathbf{P}_1 = (\varepsilon_1 - \varepsilon_0)\mathbf{E} \quad \mathbf{P}_2 = (\varepsilon_2 - \varepsilon_0)\mathbf{E}$$

and surface charge densities throughout

(2) $$\sigma_1 = \mathbf{P}_1 \cdot \mathbf{n} \qquad \sigma_2 = \mathbf{P}_2 \cdot \mathbf{n}$$

On the surface charge on the fluid side of the fluid-particle surface influences electric field in particle and on the surface charge on the particle side electric field in fluid. Both electric fields on both sides of particle surface are given by

(3) $$\mathbf{E}_1 = E_{1x}\mathbf{e}_x + E_{1y}\mathbf{e}_y \qquad \mathbf{E}_2 = E_{2x}\mathbf{e}_x + E_{2y}\mathbf{e}_y$$

Components x and y of surface stress $\mathbf{f}_2$ acting on surface charge density σ_1 by electric field $\mathbf{E}_2$ have the form:

(4) $$f_{2x} = \varepsilon_2\varepsilon_0\left[0.5\left(E_{2x}^2 - E_{2y}^2\right)n_x + E_{2x}E_{2y}n_y\right]$$

(5) $$f_{2y} = \varepsilon_2\varepsilon_0\left[0.5\left(E_{2y}^2 - E_{2x}^2\right)n_x + E_{2x}E_{2y}n_y\right]$$

On the other side components x and y of surface stress $\mathbf{f}_1$ acting on surface charge density σ_2 by electric field $\mathbf{E}_1$ have the form:

(6) $$f_{1x} = \varepsilon_1\varepsilon_0\left[0.5\left(E_{1x}^2 - E_{1y}^2\right)n_x + E_{1x}E_{1y}n_y\right]$$

(7) $$f_{1y} = \varepsilon_1\varepsilon_0\left[0.5\left(E_{1y}^2 - E_{1x}^2\right)n_x + E_{1x}E_{1y}n_y\right]$$

Total stress acting on both particles is given by

(8) $$F_x = \oint_{S_2} f_{2x}dx + \oint_{S_1} f_{1x}dx$$

(9) $$F_y = \oint_{S_2} f_{2y}dx + \oint_{S_1} f_{1y}dx$$

The plus sign results from the direction of integration on the surface S_1, which is opposite to direction of integration along side S_2. One has to mention that signs components F_x and F_y depends on the integration direction.

On figures 2 and 3 x- and y-components of the electric field along particle perimeter are shown. One can see increase of the both component in the vicinity of the neighbouring particle. This occurs at around $10\mu\mathrm{m}$ in left particle perimeter.

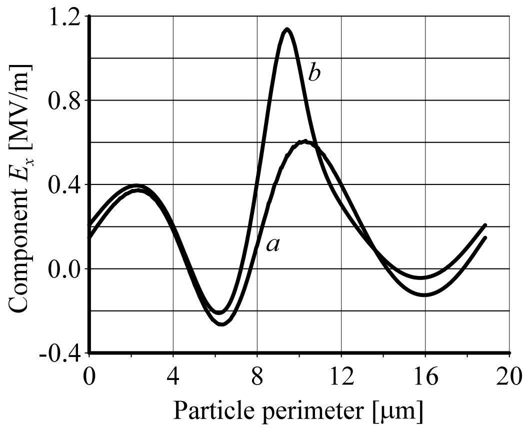

Fig.2. Component E_x of the electric field. Before neighbouring particle was placed (a) and after it was placed (b).

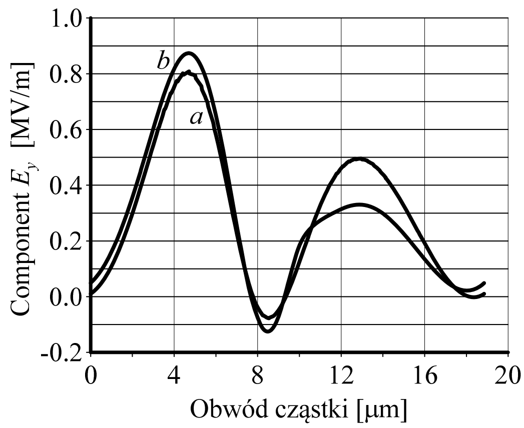

Fig.3. Component E_y of the electric field. Before neighboring particle was placed (a) and after it was placed (b).

Such increase in electric field strength has to cause induction of the greater charge density on surfaces of both particles (figures 4 and 5). Charge density increased from $21\mu\mathrm{C/m^2}$ do $40\mu\mathrm{C/m^2}$ Integral of this charge density and electric field along particle surface gives total force acting on particle.

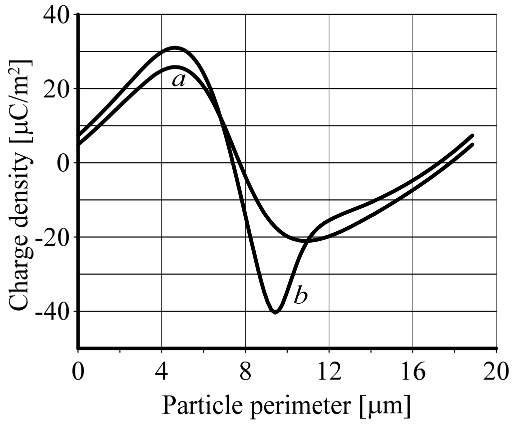

Fig.4. Distribution of the surface charge density on the left particle. Before neighboring particle was placed (a) and after it was placed (b).

Greater values of charge densities in the region of neighboring particle has to cause increase surface stress on this boundary segment. One can see this clearly on figures 5 and 6 for the fluid side. In the figure 5 x-component stress increased 8-times while y-component increased only on 40%. This shows that there exists a force, which attracts both particles. The component f_{1x} has negative value, because unite normal vector by definition is directed into the particle.

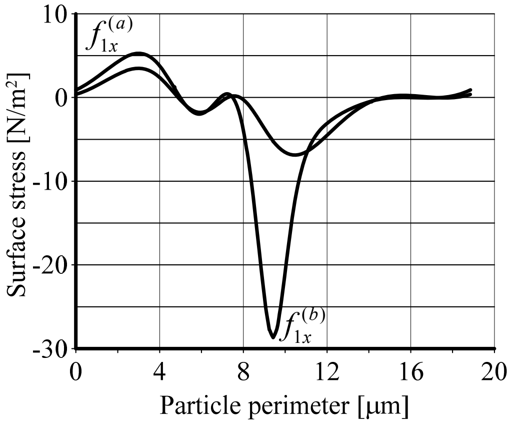

Fig.5. Change of x component surface stress distribution on the fluid side. Before neighbouring particle was placed (a) and after it was placed (b).

Another way to calculate surface stress densities is to use following formula

(10) $$f_x^{(1)} = \frac{1}{2}\left(\varepsilon_2 - \varepsilon_1\right)\left(\frac{\varepsilon_1}{\varepsilon_2}E_{1n}^2 + E_{1t}^2\right)n_x$$

(11) $$f_y^{(1)} = \frac{1}{2}\left(\varepsilon_2 - \varepsilon_1\right)\left(\frac{\varepsilon_1}{\varepsilon_2}E_{1n}^2 + E_{1t}^2\right)n_y$$

and

(12) $$F_x^{(1)} = \oint_{S_1} f_x^{(1)} ds \qquad F_y^{(1)} = \oint_{S_1} f_y^{(1)} ds$$

In figures 7 and 8 surface stresses are shown but on the particle side. One can observe that the values of these stresses are almost five times smaller the on the fluid side. One can however notice substantial increase f_{2y} component.

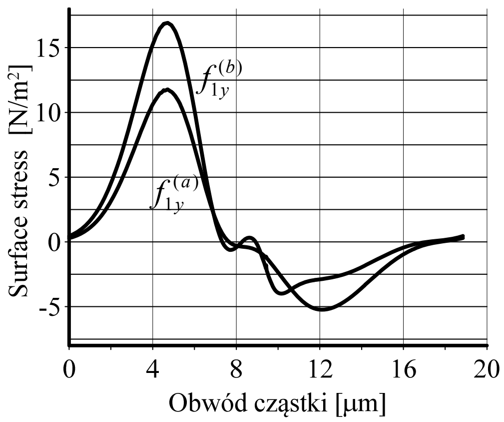

Fig.6. Change of y component surface stress distribution on the fluid side. Before neighboring particle was placed (a) and after it was placed (b).

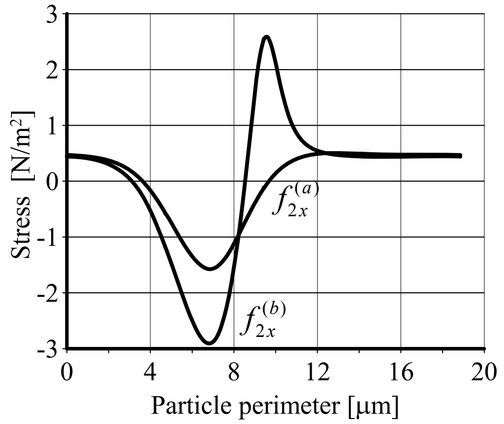

Fig.7. Change of x component surface stress distribution on the particle side. Before neighboring particle was placed (a) and after it was placed (b).

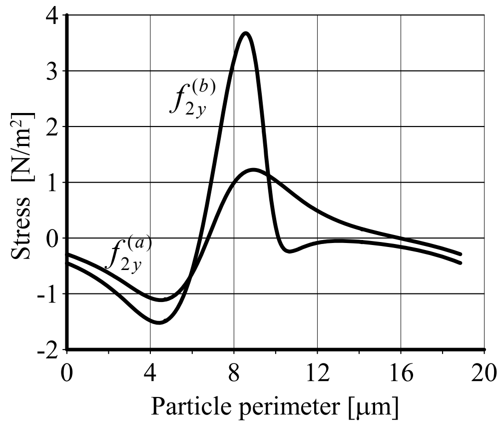

Fig.8. . Change of y component surface stress distribution on the particle side. Before neighboring particle was placed (a) and after it was placed (b).

On figures 9 for the left particle and figure 10 for the right particle, both x and y- components of the total force acting between both particles in function of mutual distance between them is presented. As one can expect, this force diminishes with the distance. The distance between particles changes from $1.5\mu\mathrm{m}$ to $21\mu\mathrm{m}$. The greatest value of both components has place, when particles are closer each other and with increasing distance these forces gradually decreases. What is interesting y-component of the force acting on the right particle has not its greater value when their mutual distance is smallest but for the value about 8μm. this is caused by the fact that in this region electric field has grater inhomogeneity.

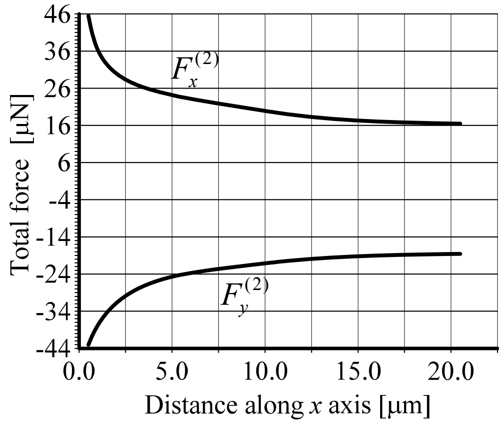

Fig.9. Change of the total x component of the force $\mathbf{F}^{(2)}$ in left particle in function of their mutual distance.

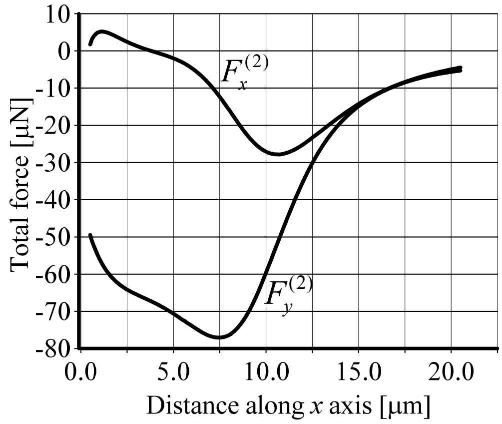

Fig.10. Change of the total x component of the force $\mathbf{F}^{(2)}$ in left particle in function of their mutual distance.

In figure 11 distribution of the surface stress distribution in vector form around left particle perimeters when the second particle is not present is shown.

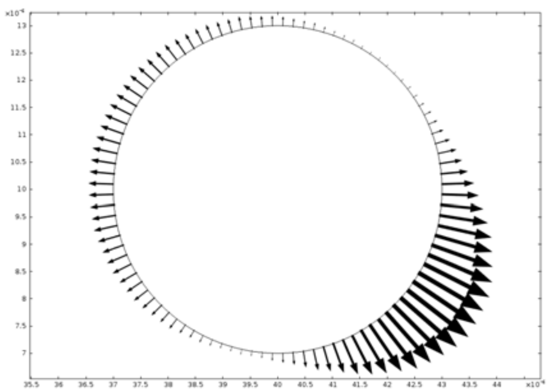

Fig.11. Surface stress distribution when left particle was alone.

This figure can be compared with the same distribution but when the second particle is present (figure 12). One can clearly see shifting of the surface stress vectors in direction of the second particle. This clearly prove that both particles attract each other.

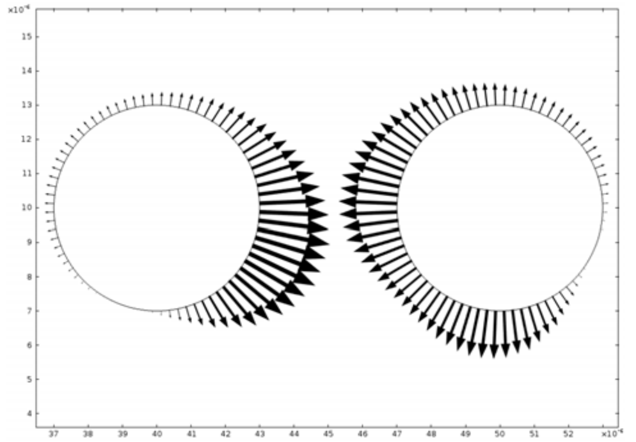

Fig.12. Change of the surface stress distribution in left particle after right particle is present.

Conclusions

In this article, two cylindrical particle in inhomogeneous electric field perpendicular to the particles was considered. Distribution of electric field, surface charge densities and surface stress are calculated using Maxwell stress tensor method.

REFERENCES

[1] Pohl, H.A., , *Dielectrophoresis*, Cambridge University Press, Cambridge, England. (1978)

[2] M. J. DeBortoli and S. J. Salon. Computation of forces and torque in electromagnetic devices using the finite element method, *ICEM'90, ,MTI*, USA, (1990), 699-705.

[3] Wang X-B., Huang Y., Becker F.F., Gascoynet P.R.C.: A unified theory of dielectrophoresis I and travelling wave dielectrophoresis, *J. Phys. D Appl. Phys*. 27, 1994, 1571-1574.

[4] Green N.G., Ramos A., Morgan H..: AC electrokinetics: a survey of sub-micrometer particle dynamics, *J. Phys. D: Appl. Phys.*, 33, 2000, 632–641..

[5] Jones T. B.: Basic Theory of Dielectrophoresis and Electrorotation, *IEEE Engineering in Medicine and Biology Magazine*, 11, 1993, 33-42.

[6] Pohl H.A., Pollock H.A., Crane J.S.: Dielectrophoretic Force: A Com-parison of Theory and Experiment, *J. Biological Phys.*, Vol. 6, 133-160, 1978.

[7] Wang X-B., Huang Y., Gascoynet P.R.C., Becker F.F.: Dielectrophoretic manipulation of particles, *IEEE Transactions on Industry Applications*, Vol. 33, no. 3, 1997, 660-669.

[8] Krawczyk A., Skoczkowski T.: Mathematical modeling of electrobio-logical interaction, *IEEE Transactions on Magnetics*, vol. 32. no. 3, 1996, 725-728.

[9] Marszalek P.: Kinetic effects of interactions between alternating electric field and layered lossy dielectric" Ph.D. Thesis, Instytut Elektrotechni-ki, Warszawa, Poland, 1991, (in Polish).

[10] Kurgan E., Gas P., Calculation of Forces Imposed on Particles in AC Dielectrophoresis, Electrical Review, 85 (2009), No. 12, 100-103..

***Authors**: Dr hab. inż. Eugeniusz Kurgan, prof. nz., AGH Akademia Górniczo-Hutnicza, Katedra Elektrotechniki i Elektroenergetyki, al. Mickiewicza 30, 30-059 Kraków, E-mail:kurgan@agh.edu.pl*
The correspondence address is: mailto:kurgan@agh.edu.pl